Journal of Aircraft
Vol. 35, No. 1, January–February 1998

Computational Study of Transonic Equivalence Rule with Lift

Shijun Luo*
Northwestern Polytechnical University, Xi'an, Shaanxi 710072, People's Republic of China
and
Lixia Wang†
General Electric Research and Development Center, Schenectady, New York 12301

The transonic equivalence rule with lift is studied computationally using the full-potential code. Two pairs of equivalent wings are designed according to the assumptions of the equivalence rule at freestream Mach number = 0.94. One pair of equivalent wings has a concorde-like planform and the other pair has a delta planform with sine tip-fairing. The computed pressure distributions in the outer flowfield of the two pairs of equivalent wings and the wave drag coefficients of the former pair are analyzed, and the equivalence rule is verified.

I. Introduction

THE steady transonic small-disturbance flows past a three-dimensional wing have been analyzed by Cheng and Hafez,[1] using the method of asymptotic expansions, leading to the establishment of the transonic equivalence rule with lift. A transonic-flow experiment, designed to study the equivalence rule with lift, was carried out by Chan.[2] The experiments succeeded in substantiating the equivalence rule with lift. However, the experimental investigations inevitably involve interaction of the shock wave and the boundary layer on the wing. Thus, an inviscid flowfield computation of the transonic flow about the wing should provide a more concrete verification of the theory of transonic equivalence rule.[3]

A computational study of the transonic equivalence rule at zero lift was provided by Caughey and Jameson.[4] The present paper attempts to study computationally the transonic equivalence rule with lift. As pointed out in Ref. 3, several requirements of the transonic equivalence rule with lift are not met in the experiments of Ref. 2. It is essential to observe the assumptions made in the theory of Ref. 1 in this computational study.

In the present paper, the theoretical results of the transonic equivalence rule with lift are first outlined. The design of two pairs of equivalent wing models for the computations is then described. The computational results are analyzed in the parametric forms defined by the equivalence rule, and the equivalence rule with lift is verified.

II. Coordinates, Wing, and Flow Parameters

The Cartesian coordinates x, y, and z are introduced with the x axis parallel to the freestream velocity U_∞ and the z axis pointing in the lift direction. They are nondimensionalized by two parameters of the wing, l and b:

$$\tilde{x} = x/l, \qquad \tilde{y} = y/b, \qquad \tilde{z} = z/b \tag{1}$$

where l is the streamwise length of the wing and may be taken as the root chord c_0, and b is the half-span of the wing.

To simplify this work, the tilde will be omitted. The ratio of b to l is denoted by λ

$$\lambda = b/l \tag{2}$$

and is referred to as the sweep parameter of the wing.

The wings considered in this paper have a symmetric plane, which is taken to be the plane $y = 0$. The spanwise outermost edges of the wing and trailing vortex sheet are defined by the local half-span at x station $a(x)$, which is nondimensionalized by b.

The upper and lower surfaces of the wing that lie close to the plane $z = 0$ are defined by

$$Z_u(x, y) = l[\alpha Z_0(x, y) + \tau Z_1(x, y)] \tag{3}$$

$$Z_l(x, y) = l[\alpha Z_0(x, y) - \tau Z_1(x, y)] \tag{4}$$

where $Z_0(x, y)$ is the generalized camber function, $Z_1(x, y)$ is the thickness function, and α and τ are the generalized camber and thickness ratios, respectively.

In the transonic equivalence rule with lift, both α and τ are assumed to be small quantities, and

$$\alpha = \mathcal{O}(\tau^{1/2}) \tag{5}$$

The sweep parameter λ, however, may take values of order one.

The reduced cross-sectional area of the wing is given by

$$S_c(x) = 2\int_{-a(x)}^{a(x)} Z_1(x, y)\, dy \tag{6}$$

The freestream Mach number is assumed to be close to 1, and

$$|1 - M_\infty^2| = \mathcal{O}(\tau) \tag{7}$$

For the similarity study of transonic small-disturbance flow, the outer transverse coordinates should be scaled by a small parameter ε

$$\eta = \varepsilon y, \qquad \zeta = \varepsilon z \tag{8}$$

where $\varepsilon \to 0$ as $\tau \to 0$. The outer flow variables are then x, η, and ζ.

Received June 8, 1996; revision received April 7, 1997; accepted for publication June 24, 1997.

*Professor, Department of Aerospace Engineering; currently Visiting Professor, Department of Mechanical and Aerospace Engineering, University of California, Irvine, CA 92697.

†Mechanical Engineer, Fluid Mechanics Program, P.O. Box 8. Member AIAA.

III. Transonic Equivalence Rule

In the theory of the transonic equivalence rule, the transonic similarity parameter is defined as

$$K = \frac{M_\infty^2 - 1}{(\gamma + 1)M_\infty^2 \tau\lambda} \tag{9}$$

where γ is the gas specific-heat ratio.

The outer transverse-coordinates scale parameter is given by the theory

$$\varepsilon = [(\gamma + 1)M_\infty^2 \tau\lambda^3]^{1/2} \tag{10}$$

Another parameter σ related to lift is introduced in the theory

$$\sigma = \frac{(\gamma + 1)^{1/2} M_\infty \alpha\lambda^{3/2}}{\tau^{1/2}} \tag{11}$$

The function related to the axial distribution of the lift on the wing is defined in the equivalence theory

$$F(x) = \int_{-a(x)}^{a(x)} [\varsigma_0(x, y)] \, \mathrm{d}y \tag{12}$$

where $[\varsigma_0(x, y)]$ is the potential jump across the wing determined by the linear transonic (or slender-body) theory, and is normalized by $\alpha U_\infty b$, and $F(x)$ signifies the lift in front of the x station of the wing.

The axial distribution function of the cross-sectional area of the equivalent body is defined as

$$S_e(x) = S_c(x) + \sigma^2 \left[\frac{F_x^2}{8\pi} \left(|\ell n \, \varepsilon| + \frac{1}{2} \right) + \frac{T(x)}{2} + \frac{E(x)}{(\gamma + 1)\lambda^2} \right] \tag{13}$$

with

$$E(x) = \frac{1}{4\pi} \int_{-a(x)}^{a(x)} \int_{-a(x)}^{a(x)} [\varsigma_0(x, s)]_s [\varsigma_0(x, y)]_y \, \ell n \frac{1}{|y - s|} \, \mathrm{d}s \, \mathrm{d}y \tag{14}$$

$$T(x) = \frac{1}{4\pi} \int_{-a(x)}^{a(x)} \int_{-a(x)}^{a(x)} [\varsigma_0(x, s)]_x [\varsigma_0(x, y)]_x \, \ell n \frac{1}{|y - s|} \, \mathrm{d}s \, \mathrm{d}y \tag{15}$$

where the subscripts x, y, and s refer to partial derivatives, and the second term of the expression for $S_e(x)$ is the contribution resulting from lift.

The transonic equivalence rule with lift states that the outer flow structure at a given K, including the pressure distribution and the wave drag, is identical in their reduced forms as long as the functions $\sigma F(x)$ and $S_e(x)$ remain the same. The reduced pressure coefficient in the outer flowfield is $c_p/\tau\lambda$, and the reduced wave drag coefficient is $c_{D_w}/\tau^2\lambda$. Thus, the equivalence rule can be expressed for the reduced pressure coefficient

$$\frac{c_p}{\tau\lambda} = f(x, \eta, \zeta, K) \tag{16}$$

and for the reduced wave drag coefficient

$$c_{D_w}/\tau^2\lambda = g(K) \tag{17}$$

The latter equation is derived by the conservation law of momentum. The wave drag of wing is evaluated as a far-field cylindrical surface integral of axial-momentum flux. It is noted that Eq. (17) is different from that given by Eq. (5.2) of Ref. 1, which in the present notation becomes

$$\frac{c_{D_w}}{\tau^2 \lambda M_\infty^2} = g(K) \tag{18}$$

IV. Choice of Potential Jump Function

To design equivalent wings, the normalized potential jump function $[\varsigma_0(x, y)]$ is chosen according to the assumptions used in the analyses of Ref. 1. The assumptions are that, along the leading edge of the wing, the function and its partial derivatives with respect to x and y vanish. The choice is

$$[\varsigma_0(x, y)] = \frac{2}{3} a(x) \left[1 - \frac{y^2}{a^2(x)} \right]^{3/2} \tag{19}$$

In the theory of Ref. 1, the generalized camber function $Z_0(x, y)$ is related to the potential jump function as given by the linear transonic theory

$$Z_{0x}(x, y) = \frac{1}{2\pi} \mathrm{PV} \int_{-a(x)}^{a(x)} [\varsigma_0(x, y_1)]_{y_1} \frac{\mathrm{d}y_1}{y_1 - y} \tag{20}$$

where PV denotes the principal value. With the previous choice of $[\varsigma_0(x, y)]$, the function $Z_{0x}(x, y)$ is evaluated:

$$Z_{0x}(x, y) = \frac{y^2}{a^2(x)} - \frac{1}{2} \tag{21}$$

Along the leading edges of the wing, $y = a(x)$, Eq. (21) yields

$$Z_{0x}[x, a(x)] = \tfrac{1}{2} \tag{22}$$

which is positive and signifies that the wing has drooped leading edges.

Integrating Eq. (21) with respect to x yields

$$Z_0(x, y) = y^2 \int \frac{\mathrm{d}x}{a^2(x)} - \frac{x}{2} + C(y) \tag{23}$$

where $C(y)$ is a function to be determined by assuming appropriate geometric conditions on the wing.

With the expression of $[\varsigma_0(x, y)]$ [Eq. (19)], the lift-related functions $F(x)$, $E(x)$, and $T(x)$ are evaluated

$$F(x) = (\pi/4)a^2(x) \tag{24}$$

$$E(x) = (\pi/24)a^2(x) \tag{25}$$

$$T(x) = (\pi/16)a^2(x)a'^2(x) \left\{ \ell n \left[\frac{2}{a(x)} \right] + \frac{1}{8} \right\} \tag{26}$$

where the prime symbol denotes derivative, and the function $S_e(x)$ becomes

$$S_e(x) = S_c(x) + \frac{\pi\sigma^2 a^2(x)}{24} \times \left\{ \frac{3}{4} a'^2(x) \left[|\ell n \, \varepsilon| + \ell n \frac{2}{a(x)} + \frac{5}{8} \right] + \frac{1}{(\gamma + 1)\lambda^2} \right\} \tag{27}$$

The thickness function $Z_1(x, y)$ is to be determined for equivalent wings by keeping $S_e(x)$ the same.

V. Design of Equivalent Wings

Equivalent wing models are designed for computations. The freestream Mach number and the gas specific-heat ratio take the same values for equivalent wings. The transonic similarity parameter K [Eq. (9)] should be the same for equivalent wings. Therefore

$$\tau_1\lambda_1 = \tau_2\lambda_2 \tag{28}$$

where the subscripts 1 and 2 denote two equivalent wings.

As the lift function $F(x)$ is the same for two equivalent wings, the lift parameter σ [Eq. (11)] should be the same for the two wings. With the combination of Eq. (28), this requirement gives

$$\alpha_1\lambda_1^2 = \alpha_2\lambda_2^2 \tag{29}$$

Under condition (28), the equivalence rule for the reduced pressure coefficient (16) becomes

$$c_{p1}(x, \eta, \zeta) = c_{p2}(x, \eta, \zeta) \tag{30}$$

and the equivalence rule for the reduced wave drag coefficient [Eq. (17)] becomes

$$\frac{c_{D_{w1}}}{c_{D_{w2}}} = \frac{\lambda_2}{\lambda_1} \tag{31}$$

The coordinates of the upper and lower surfaces of the two equivalent wing models are evaluated by Eqs. (3) and (4). The generalized camber function $Z_0(x, y)$ is the same for the two wings, as given by Eq. (23). The thickness function $Z_1(x, y)$ is different for the two wings. The thickness function of one wing, $Z_{11}(x, y)$, is chosen as that of the NACA four-digit wing sections[5]:

$$Z_{11}(x, y) = \frac{1 - x_{le}(y)}{0.2}(0.29690x_1^{1/2} - 0.12600x_1 - 0.35160x_1^2 + 0.28430x_1^3 - 0.10150x_1^4) \tag{32}$$

where

$$x_1 = \frac{x - x_{le}(y)}{1 - x_{le}(y)} \tag{33}$$

$$x_{le}(y) = \frac{1}{\pi}\arccos(1 - 2y) \tag{34}$$

The thickness function of the other wing is calculated from having the same axial distribution of cross-sectional area of the equivalent body, $S_e(x)$ [Eq. (27)]

$$Z_{12}(x, y) = Z_{11}(x, y) + h(x)[a(x) - y] \tag{35}$$

where

$$h(x) = \frac{\pi(\gamma + 1)M_\infty^2\alpha_1^2\lambda_1^3}{48\tau_1}\left[\frac{3a'^2(x)}{4}(|\ell n\,\varepsilon_1| - |\ell n\,\varepsilon_2|) + \frac{1}{\gamma + 1}\left(\frac{1}{\lambda_1^2} - \frac{1}{\lambda_2^2}\right)\right] \tag{36}$$

VI. Concorde-Like Wing

The leading-edge contour function $a(x)$ is chosen to ensure $F'(x)$ vanishing at the upstream and downstream ends of the wing. Two different choices of $a(x)$ are made. The first choice is a concorde-like wing

$$a(x) = \tfrac{1}{2}(1 - \cos\pi x) \tag{37}$$

The trailing edge of the wing is taken as a straight line through the wing tips. The planform thus formed is concorde-like, as shown in Fig. 1.

Table 1 Equivalent concorde-like wings

Wing	λ	τ	α	ε
1	$\frac{2}{3}$	0.09	0.3	0.2378
2	1	0.06	0.1333	0.3567

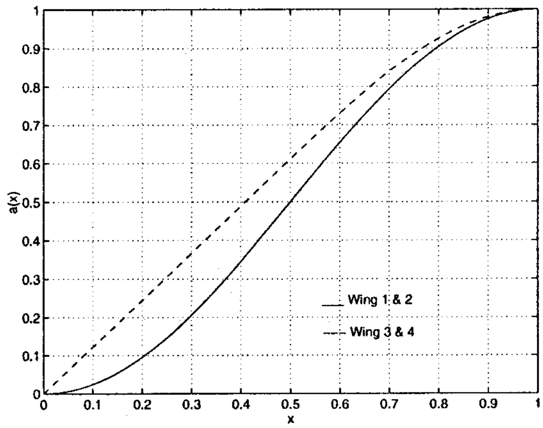

Fig. 1 Planforms of equivalent wings.

For the concorde-like wing [Eq. (37)], the generalized camber function $Z_0(x, y)$ becomes

$$Z_0(x, y) = -\frac{4y^2}{3\pi}\left(1 + \frac{1}{1 - \cos\pi x}\right)\cot\frac{\pi x}{2} - \frac{x}{2} + C(y) \tag{38}$$

It is reasonable to assume that all midpoints of the local chords lie on the plane $z = 0$. The midpoint of the local chord is at

$$x_m(y) = \tfrac{1}{2}[1 + (1/\pi)\arccos(1 - 2y)] \tag{39}$$

The condition that $Z_0(x, y)$ vanishes at $x = x_m(y)$ yields

$$C(y) = \frac{4y^2}{3\pi}\left[1 + \frac{1}{1 - \cos\pi x_m(y)}\right]\cot\frac{\pi x_m(y)}{2} + \frac{x_m(y)}{2} \tag{40}$$

According to Eqs. (28) and (29), the first pair of equivalent wing models are designed. Their parameters are listed in Table 1, where $M_\infty = 0.94$ and $\gamma = 1.4$. The preceding values of ε are not as small as the equivalence rule requires. However, it would provide a verification of the application extent of the equivalence rule. The two wing models have the same transonic similarity parameter K [Eq. (9)] and the same lift parameter σ [Eq. (11)]

$$K = -0.9148, \qquad \sigma = 0.7927 \tag{41}$$

VII. Delta Wings with Sine Tip-Fairing

The second choice of the leading-edge contour function $a(x)$ is delta wing with sine tip-fairing

$$a(x) = (b_0/b)x \tag{42}$$

for $0 \le x \le x_0$, and

$$a(x) = \frac{b_0}{b}\left[x_0 + \frac{2}{\pi}(1 - x_0)\sin\left(\frac{\pi}{2}\frac{x - x_0}{1 - x_0}\right)\right] \tag{43}$$

for $x_0 \le x \le 1$, where x_0 is the x coordinate of the upstream

Table 2 Equivalent delta wings with sine tip-fairing

Wing	λ	τ	α	ε
3	0.4725	0.09	0.3	0.1419
4	0.8183	0.05196	0.1	0.2457

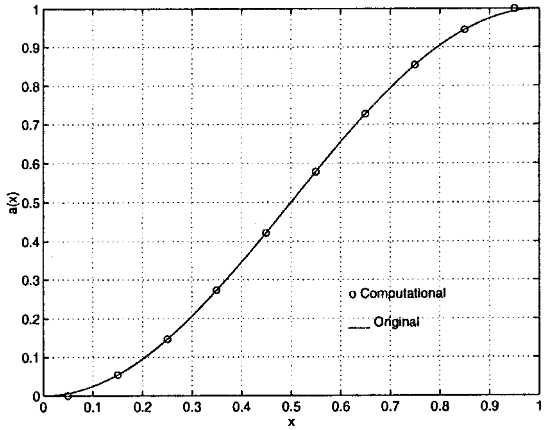

Fig. 2 Computational planform of concorde-like wings.

endpoint of sine tip-fairing, and b_0 is the semispan of a wing without tip-fairing

$$b/b_0 = x_0 + (2/\pi)(1 - x_0) \tag{44}$$

The trailing edge of the wing is taken as a straight line through the wing tips. The planform for $x_0 = 1/2$ is shown in Fig. 1.

For the delta wing with sine tip-fairing, the generalized camber function $Z_0(x, y)$, [Eq. (23)], becomes

$$Z_0(x, y) = -\left(\frac{b}{b_0}\right)^2 \frac{y^2}{x} - \frac{x}{2} + C_1(y) \tag{45}$$

for $0 \le x \le x_0$, and

$$\begin{aligned} Z_0(x, y) = {} & \left(\frac{2by}{\pi b_0}\right)^2 \left\{\frac{(1 - x_0)^2}{x_0^2 - (4/\pi)^2(1 - x_0)^2}\right. \\ & \times \left[\frac{\sin \xi}{x_0 + (2/\pi)(1 - x_0)\cos \xi} - \frac{1}{x_0}\right] \\ & - \frac{\pi x_0(1 - x_0)}{[x_0^2 - (4/\pi)^2(1 - x_0)^2]^{3/2}} \arctan \left[\frac{x_0 - (2/\pi)(1 - x_0)}{x_0 + (2/\pi)(1 - x_0)}\right]^{1/2} \\ & \times \left(\tan \frac{\xi}{2} - 1\right) - \left.\frac{1}{x_0}\right\} - \frac{x}{2} + C_1(y) \end{aligned} \tag{46}$$

for $x_0 \le x \le 1$, where

$$\xi = \frac{\pi}{2} \frac{1 - x}{1 - x_0} \tag{47}$$

The integration constant $C_1(y)$ in Eqs. (45) and (46) is determined by the condition that $Z_0(x, y)$ vanishes at all the midpoints of local chords of the wing. For the present study, the location of the upstream end of tip-fairing is taken as

$$x_0 = \tfrac{1}{2} \tag{48}$$

For this case

$$C_1(y) = \left(\frac{b}{b_0}\right)^2 \frac{y^2}{x_m(y)} + \frac{x_m(y)}{2} \tag{49}$$

Table 3 Computed drag coefficients

Wing	c_D	c_{D_i}	c_{D_w}
1	0.02124	0.01147	0.00977
2	0.00928	0.00375	0.00553

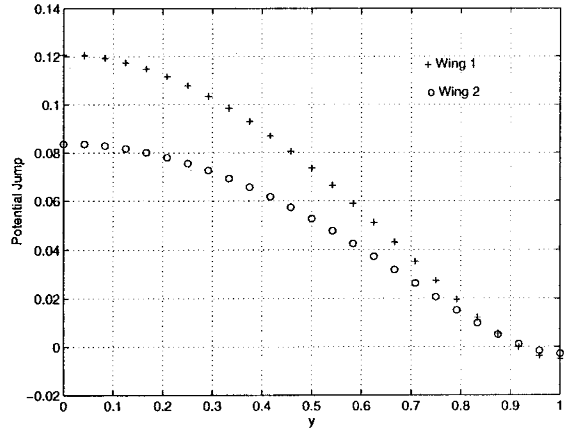

Fig. 3 Computed velocity potential jumps along trailing edge.

where $x_m(y)$ locates the midpoint of the local chord of the wing

$$x_m(y) = \frac{1 + (b/b_0)y}{2} \tag{50}$$

for $0 \le y \le b_0/2b$, and

$$x_m(y) = \frac{1 + x_0}{2} + \frac{1 - x_0}{\pi} \arcsin\left(\frac{\pi}{2}\frac{b}{b_0}\frac{y - x_0}{1 - x_0}\right) \tag{51}$$

for $b_0/2b \le y \le 1$.

The parameters of the second pair of equivalent wings are listed in Table 2, where $M_\infty = 0.94$ and $\gamma = 1.4$. The transonic similarity parameter K [Eq. (9)] and the lift parameter σ [Eq. (11)] are the same for the two wings

$$K = -1.2909, \qquad \sigma = 0.4729 \tag{52}$$

VIII. Computations

The full potential flow around the four wing models at $M_\infty = 0.94$ are calculated by a multigrid version of Flo-27, which is based on the finite volume method of Jameson and Caughey.[6,7] The fine grid is $160 \times 32 \times 24$ in x, y, and z directions, respectively. The multigrid level is three. The convergence tolerance required is that the average residual is reduced by 3×10^{-3}. Under this condition, the solutions are generally converged to four significant figures in force coefficients.

The Flo-27 code requires that the taper ratio of the computed wing not be zero, and the leading-edge sweep angle should not be close to 90 deg. Accordingly, the concorde-like wing planform is modified at both root and tip, and the delta wing planform is modified at tip. The root section of the concorde-like wing models is replaced by the section with leading edge at $x = 0.05$. And a tip section is created for both wing planforms by using the section with leading edge at $x = 0.95$. The computational planform of the concorde-like wing models is shown in Fig. 2, as compared with the original planform. It is seen that the overall modifications to the wing geometries are rather minor.

The computation gives the velocity potential and pressure coefficient at all grid points in the flowfield around the wing, and the lift, pitching moment coefficient, and pressure drag

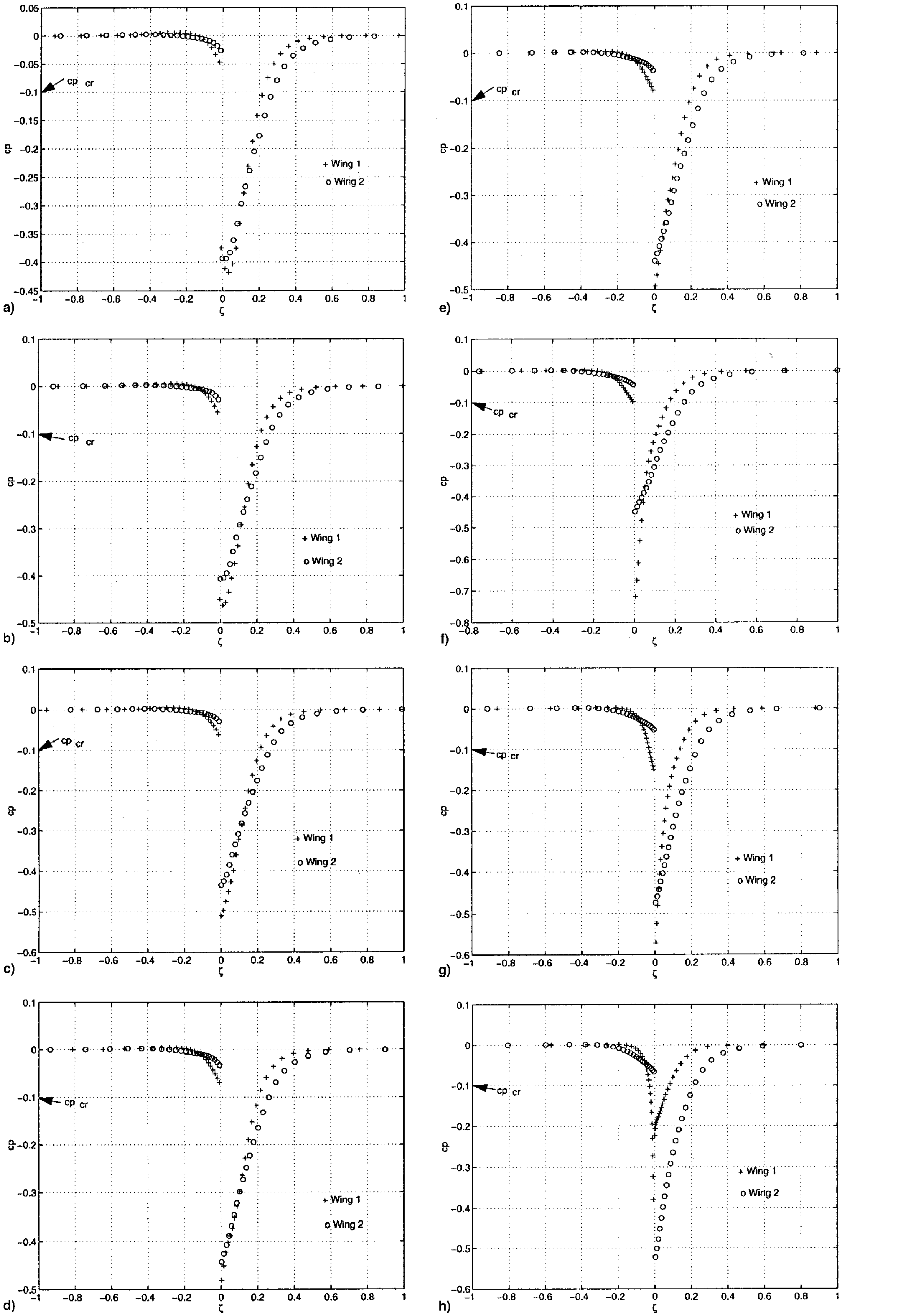

Fig. 4 Field pressure distributions of equivalent concorde-like wings. η = a) 0, b) 0.0297, c) 0.0595, d) 0.0892, e) 0.1189, f) 0.1486, g) 0.1784, and h) 0.2081.

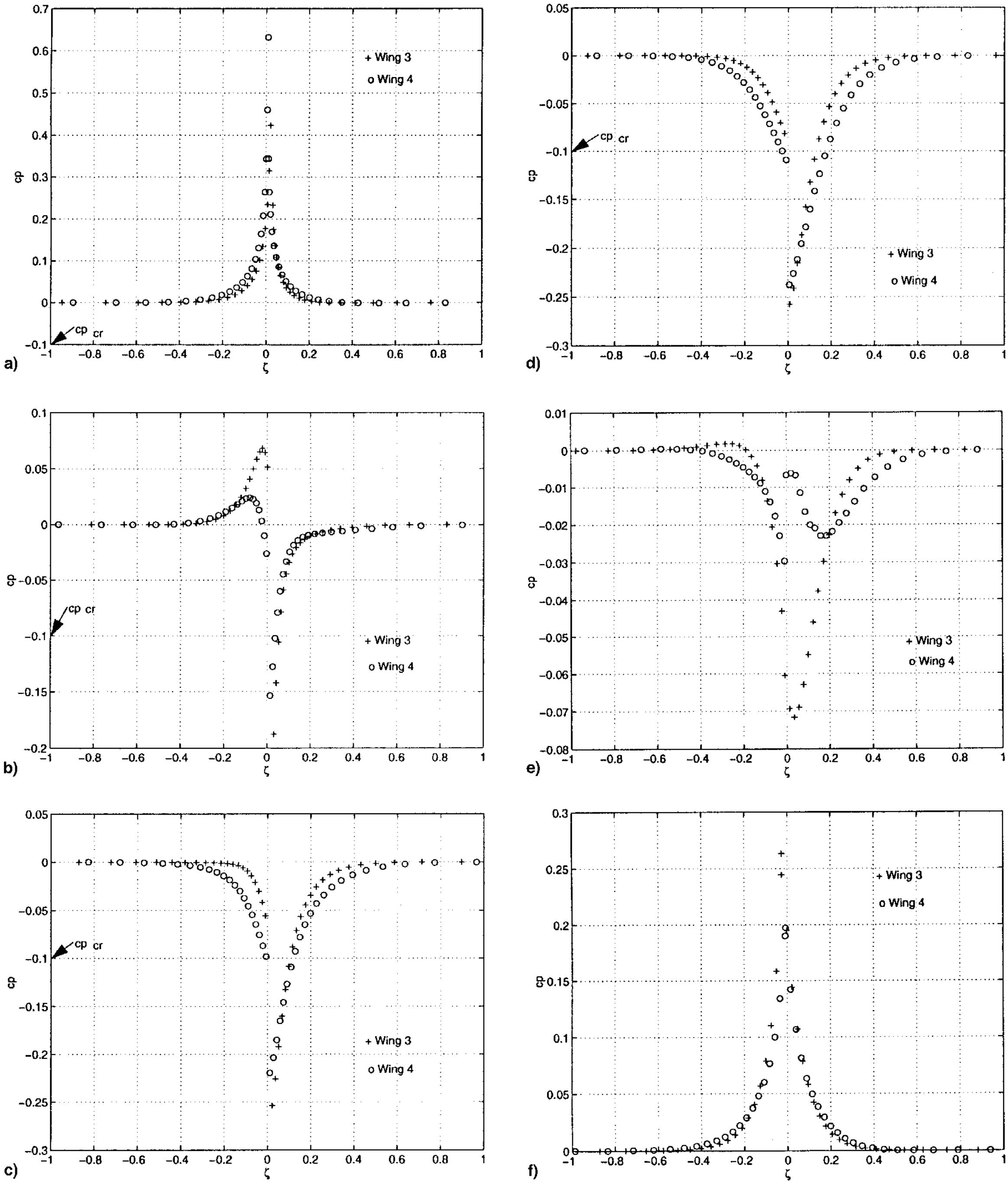

Fig. 5 Field pressure distributions of equivalent delta wings with sine tip-fairing. x = a) 0, b) 0.2, c) 0.4, d) 0.6, e) 0.8, and f) 1.

coefficient of the wing. To find the wave drag, vortex or induced drag is first calculated from the computed potential jump along the wing trailing edge $[\phi(y)]$, and it is then subtracted from the computed pressure drag coefficient c_D.

The vortex drag coefficient c_{D_i} is evaluated by the following formula[8]:

$$c_{D_i} = \frac{\pi b^2}{S} \sum_{n=1}^{N} n A_n^2 \tag{53}$$

where A_n is the reduced coefficient of the sine series of the potential jump

$$[\phi(y)] = 2bU_\infty \sum_{n=1}^{N} A_n \sin n\theta \tag{54}$$

with θ defined by the variable transformation

$$y = \cos\theta \tag{55}$$

S is the wing planform area that is for the concorde-like wing

$$S = bc_0 \tag{56}$$

The computed velocity potential jumps along the trailing edge of the concorde-like wing models are shown in Fig. 3. Note that they do not vanish at the tips of the wings, as should be occurring. This may be caused by a bad behavior of the grids observed in wing-tip regions, associated with very large leading-edge sweep and very small taper ratio of the computed wings. Thus, the velocity potential jumps are set to be zero at the wing tips in calculating the vortex drag. With $N = 40$, the results are converged to four significant figures in vortex drag coefficient.

The computed various drag coefficients are listed in Table 3. The wave drag coefficients of wings 3 and 4 are too small to be calculated accurately and, thus, are not included here.

IX. Verification

The computed pressure coefficients and wave drag coefficients are used to verify the transonic equivalence rule with lift, which is expressed by Eqs. (30) and (31) for the equivalent wing models. Equation (30) states that the pressure coefficient distributions in terms of the outer scaled variables are identical in the outer flowfield. Equation (31) states that the wave drag coefficient ratio of the two wings is equal to the reciprocal of the corresponding λ ratio.

The computed pressure coefficients as correlated with the scaled outer variables x, η, and ζ are plotted at different η and x stations. Figure 4 gives the field pressure distributions around wings 1 and 2 at $x = 0.8$ and various spanwise stations. Figure 5 gives the field pressure distributions around wings 3 and 4 in the symmetric plane at various x stations. It is seen that the pressure coefficient distributions of the two wing models are generally identical in the outer flowfield, or when ζ is not close to zero.

From the computational results of Table 3, the wave drag coefficient ratio of wings 1 and 2 is

$$\frac{c_{D_{w1}}}{c_{D_{w2}}} = \frac{0.00977}{0.00553} = 1.77 \tag{57}$$

From the equivalence rule, it should be the reciprocal of the corresponding λ ratio of the two wings

$$\lambda_2/\lambda_1 = 1/\tfrac{2}{3} = 1.50 \tag{58}$$

The computed ratio is deviated from that predicted by the equivalence rule by 15%.

The deviations between the computational results and those predicted by the equivalence rule may be mainly because the designed values of parameter ε, as shown in Tables 1 and 2, are not small enough. However, it does show that the transonic equivalence rule with lift is a good approximation for engineering applications, even when ε is about 0.3.

X. Concluding Remarks

The transonic equivalence rule with lift has been studied computationally using a multigrid version of the full potential code, Flo-27. Equivalent wing models are designed such that the assumptions made in the theoretical rule are satisfied. One pair of equivalent wings has a concorde-like planform and the other pair has a delta planform with sine tip-fairing. The equivalent wings have different values of aspect ratio, thickness ratio, and generalized camber ratio. The freestream Mach number is $M_\infty = 0.94$ for all computations. The computed outerfield pressure distributions and wave drags of the equivalent wings agree well with the theoretical rules, even when the small-disturbance parameter ε is as high as 0.3.

Acknowledgments

This study was partially supported by the National Science Foundation U.S.-China Cooperative Research Program, Award 9017252 (1990–1992). The computations were performed at the Sibley School of Mechanical and Aerospace Engineering of Cornell University. The authors express their appreciation for the helpful suggestions offered by H. K. Cheng and D. A. Caughey. S. Luo acknowledges the generous support from the Department of Aerospace Engineering of the University of Southern California.

References

[1]Cheng, H. K., and Hafez, M. M., "Transonic Equivalence Rule: A Nonlinear Problem Involving Lift," *Journal of Fluid Mechanics*, Vol. 72, Pt. 1, Nov. 1975, pp. 161–187.

[2]Chan, Y. Y., "An Experimental Study of the Transonic Equivalence Rule with Lift," Canada National Aeronautical Establishment, Aeronautical Rept. LR-609, National Research Council, March 1982.

[3]Cheng, H. K., "Transonic Equivalence Rule: Unsolved Aspects of Asymptotic and CFD Studies," Dept. of Aerospace Engineering, Univ. of Southern California, Aerospace Engineering, Los Angeles, CA, June 1988.

[4]Caughey, D. A., and Jameson, A., "Numerical Calculation of Transonic Potential Flow About Wing-Body Combinations," *AIAA Journal*, Vol. 17, No. 2, 1979, pp. 175–181.

[5]Abbott, I. H., and Von Doenhoff, A. E., "Theory of Wing Sections, Including a Summary of Airfoil Data," Dover, New York, 1959, p. 113.

[6]Jameson, A., and Caughey, D. A., "A Finite Volume Method for Transonic Potential Flow Calculations," *Proceedings of the 3rd Computational Fluid Dynamics Conference* (Albuquerque, NM), 1977, pp. 35–54.

[7]Caughey, D. A., "Multi-Grid Calculation of Three-Dimensional Transonic Potential Flows," *Applied Mathematics and Computation*, Vol. 13, Nos. 3 and 4, 1983, pp. 241–260.

[8]Ashley, H., and Landahl, M., *Aerodynamics of Wings and Bodies*, Dover, New York, 1965, p. 137.